

TESS REVEALS THAT THE NEARBY PISCES–ERIDANUS STELLAR STREAM IS ONLY 120 MYR OLD

JASON L. CURTIS,^{1,*} MARCEL A. AGÜEROS,¹ ERIC E. MAMAJEK,^{2,3} JASON T. WRIGHT,⁴ AND JEFFREY D. CUMMINGS⁵

¹*Department of Astronomy, Columbia University, 550 West 120th Street, New York, NY 10027, USA*

²*Jet Propulsion Laboratory, California Institute of Technology, M/S 321-100, 4800 Oak Grove Drive, Pasadena, CA 91109, USA*

³*Department of Physics & Astronomy, University of Rochester, Rochester, NY 14627, USA*

⁴*Center for Exoplanets and Habitable Worlds, Department of Astronomy & Astrophysics, The Pennsylvania State University, 525 Davey Laboratory, University Park, PA 16802, USA*

⁵*Center for Astrophysical Sciences, Johns Hopkins University, 3400 N. Charles Street, Baltimore, MD 21218, USA*

(Accepted May 24, 2019)

Submitted to *The Astronomical Journal*

ABSTRACT

Pisces–Eridanus (Psc–Eri), a nearby ($d \simeq 80\text{--}226$ pc) stellar stream stretching across $\approx 120^\circ$ of the sky, was recently discovered with *Gaia* data. The stream was claimed to be ≈ 1 Gyr old, which would make it an exceptional discovery for stellar astrophysics, as star clusters of that age are rare and tend to be distant, limiting their utility as benchmark samples. We test this old age for Psc–Eri in two ways. First, we compare the rotation periods for 101 low-mass members (measured using time series photometry from the *Transiting Exoplanet Survey Satellite*, *TESS*) to those of well-studied open clusters. Second, we identify 34 new high-mass candidate members, including the notable stars λ Tauri (an Algol-type eclipsing binary) and HD 1160 (host to a directly imaged object near the hydrogen-burning limit). We conduct an isochronal analysis of the color–magnitude data for these highest-mass members, again comparing our results to those for open clusters. Both analyses show that the stream has an age consistent with that of the Pleiades, i.e., ≈ 120 Myr. This makes the Psc–Eri stream an exciting source of young benchmarkable stars and, potentially, exoplanets located in a more diffuse environment that is distinct from that of the Pleiades and of other dense star clusters.

Keywords: open clusters: individual (Pisces–Eridanus Stream, Pleiades, Praesepe, NGC 6811) — stars: evolution — stars: rotation — stars: individual (HD 1160 B, TOI 451)

1. INTRODUCTION

Star clusters at least 1 Gyr in age are rare, and tend to be located at large distances from Earth (e.g., Dias et al. 2002; Kharchenko et al. 2005). This is a shame, because such clusters serve as critical benchmarks for stellar astrophysics. Recently, Meingast et al. (2019) announced the discovery of a stellar stream that stretches 120° across the sky, and spans ≈ 400 pc in space. This discovery was made possible by the precise astrometry, radial velocities (RVs), and photometry included in the *Gaia* mission’s second data release (DR2; Gaia Collaboration et al. 2018a). Discovery of the Pisces–

Eridanus stream (Psc–Eri)¹ was somewhat of a surprise

¹ The stream was undesignated in Meingast et al. (2019). The authors of the discovery paper suggested the name “MAF-1” for the stream (S. Meingast, priv. comm.); however, this is very different from the nomenclature for nearby associations (e.g. de Zeeuw et al. 1999; Torres et al. 2008). This acronym could be confused with two acronyms already in the Dictionary of Nomenclature of Celestial Objects (<http://cds.u-strasbg.fr/cgi-bin/Dic-Simbad>; Lortet et al. 1994)—[MAF2004] and [MAF2009]—the latter of which is used for members of the open cluster NGC 7062 (Molenda-Žakowicz et al. 2009), or as an abbreviation of the Maffei galaxies or Maffei Group of galaxies (e.g. Fingerhut et al. 2007). Two of the main concentrations of the stream’s members are in the constellations Eridanus (clump 1) and Pisces (clump 3), and the group’s convergent point ($\alpha, \delta \simeq 42^\circ 6, -20^\circ 0$; ICRS) lies in Eridanus as well. As we find in our analysis that the group is more analogous to an older version of an OB association, similar to other expansive nearby stellar associations like Sco–Cen and Tuc–Hor, we combine the two prominent constellation names and refer to it as the “Pisces–Eridanus stream” or Psc–Eri.

Corresponding author: Jason Lee Curtis
jasoncurtis.astro@gmail.com

* NSF Astronomy and Astrophysics Postdoctoral Fellow

Table 1. Ages and distance moduli for notable benchmark star clusters with rotation data.

Name	$m - M$	Age (Gyr)	Age Reference
Pleiades	5.67	0.120	Stauffer et al. (1998) ^b
Praesepe	6.35	0.670	Douglas et al. (2019)
Hyades	3.37	0.730	Douglas et al. (2019)
NGC 6811	10.20	1.0	Curtis et al. (2019)
NGC 752	8.20	1.4	Agüeros et al. (2018)
Ruprecht 147	7.40	2.7	Torres et al. (2018)
M67	9.72	4.0	Önehag et al. (2011)

NOTE—These distance moduli only account for distance, and do not include visual extinction.

^aThe Pleiades age has been constrained with lithium depletion boundary to 125–130 Myr by Stauffer et al. (1998) and 115 ± 5 Myr by Dahm (2015). Recent isochrone analyses by Gossage et al. (2018) found 110–160 Myr; Cummings & Kalirai (2018) found 115–135 Myr. We adopt 120 Myr for this work.

given its combination of old age (≈ 1 Gyr) and proximity ($d = 129 \pm 32$ pc from Earth; median and standard deviation of the 256 published members; the full range is $d \simeq 80$ –226 pc). For context, we list the distance moduli for notable benchmark open clusters along with their ages in Table 1. Figure 1 plots the age and distance to a selection of clusters with measured rotation periods (P_{rot}), which further highlights how remarkable and useful a 1 Gyr cluster this close to Earth would be.

If Psc–Eri’s age is truly 1 Gyr, it would be the oldest coeval stellar population within 300 pc. This would open up many avenues for research that are difficult or impossible to pursue with the 1 Gyr-old benchmark cluster NGC 6811 (Sandquist et al. 2016; Curtis et al. 2019), currently the only open cluster of this age we have been able to study in detail. For example, Meibom et al. (2013) discovered two sub-Neptune exoplanets in NGC 6811, but these are too faint for efficient RV follow-up. It is also challenging to measure chromospheric Ca II H & K activity indices for FGK stars in NGC 6811: those stars are faint (a solar twin is $V \approx 15$), and the interstellar Ca II H & K contamination is difficult to mitigate (Curtis 2017). Finally, Psc–Eri could be an interesting test case for demonstrating the chemical tagging technique needed for Galactic archaeology (Freeman & Bland-Hawthorn 2002).

Given the potential value of this population of stars, it is important to examine its age to see if it can serve as a benchmark for old stars. A similar exercise with the purportedly old nearby cluster Ruprecht 147 proved very fruitful (Curtis et al. 2013; Curtis 2016), while the

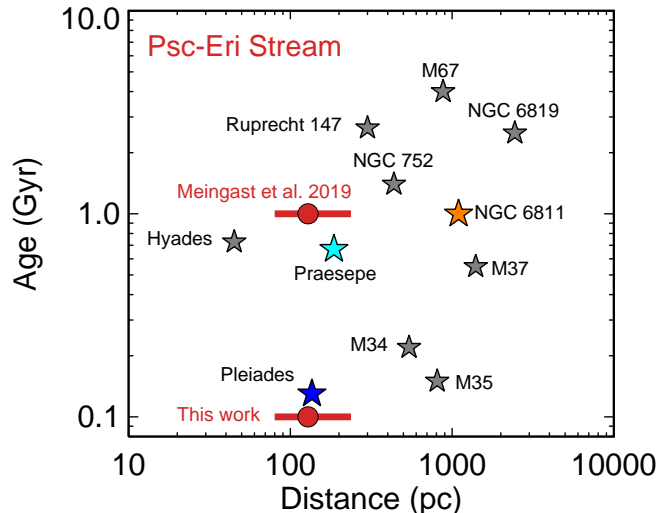


Figure 1. Age versus distance for a selection of benchmark star clusters with rotation period measurements. The distance to the Psc–Eri stream is shown as a red point marking the median and a red line showing the range. If this stream is really ≈ 1 Gyr in age, it would become a critical target for rotation/activity studies and an important benchmark for stellar astrophysics. By comparing rotation periods in Psc–Eri to those in the clusters shown as colored stars, and by re-examining its color-magnitude diagram, we demonstrate that it is closer to ~ 100 Myr old.

exploration of another candidate old cluster, Lodén 1, showed that it did not exist (Han et al. 2016).

We use gyrochronology, the age-dating method based on stellar rotation and magnetic braking (Barnes 2003; Soderblom 2010), to test the existence and coevality of the Psc–Eri stream. Coeval stars form well-defined sequences in their color–period diagrams, analogous to the main sequence in a color–magnitude diagram (CMD). But color–period sequences are much more sensitive to age, as the full sequence evolves measurably in time as stars spin down, while only the massive end of the main sequence shows significant evolution in temperature and luminosity. If the stars are coeval, a gyrochronology analysis will also yield a precise age for the Psc–Eri stream. We conduct this experiment in Section 2, where we extract and analyze light curves for 101 members of the stream observed by *TESS*. We find that the resulting P_{rot} distribution precisely overlaps the Pleiades distribution, making it ≈ 120 Myr old.

In Section 3, we reinterpret the stream’s CMD by noting that *Gaia* DR2 measured RVs for stars with $T_{\text{eff}} \lesssim 7000$ K, which biased the Meingast et al. (2019) membership census. The Psc–Eri stream’s CMD closely matches that of the Pleiades, except that its membership is truncated due to this RV bias. Combining *Gaia* DR2 data with literature RVs, we identify 22 new can-

didates that are warmer than the stars in the Meingast et al. (2019) sample, and another 12 that lack RVs but are co-moving in proper motion within 10 pc of known members. These stars closely follow the upper main sequence of the Pleiades, providing further evidence of the Psc–Eri stream’s young age. We also briefly discuss the stream’s formation in Section 3, before concluding in Section 4.

2. AGE-DATING THE PSC–ERI STREAM WITH GYROCHRONOLOGY

2.1. Rotation Period Measurements with TESS

The *Transiting Exoplanet Survey Satellite* (TESS; Ricker et al. 2015) is currently conducting a year-long photometric monitoring campaign of the southern sky. TESS scans the sky in a series of sectors for ≈ 27 d at a time. Full frame images (FFI) are recorded with a 30 m cadence. As of writing, FFI data for the first five sectors have been released to the Mikulski Archive for Space Telescopes (MAST).

Meingast et al. (2019) published a list of 256 candidates members of the Psc–Eri stream. We used the Web TESS Viewing Tool (WTV)² to identify stars observed during Sectors 1–5, and we found 154 with data from at least one sector. We downloaded 20×20 pixel cutouts of the FFI images centered on each target using the TESSut tool hosted at MAST (Brasseur et al. 2019).³ Next, we used the IDL procedure `aper.pro` from the IDL Astronomy User’s Library (Landsman 1993) to perform aperture photometry on all epochs in the image stack produced by TESScut. We used a circular aperture with a 3 pixel radius ($\approx 1'$ based on TESS’s $\approx 21''$ pixel scale).

The resulting light curves overwhelmingly showed clear spot modulation with relatively large amplitudes and short periods compared to our expectations from the 1 Gyr NGC 6811 data from *Kepler* (Curtis et al. 2019; Meibom et al. 2011b). We were able to measure P_{rot} without performing any additional calibration on these light curves. Figures 2 and 3 show examples of TESS light curves for stream members produced following this simple procedure.

2.2. The Color–Period Diagram

We measured rotation periods for 101 stars using Lomb–Scargle periodograms (Scargle 1982; Press & Rybicki 1989). After extracting each light curve and computing the periodogram, we visually inspected the results (see Figures 2 and 3) to ensure the accuracy of

our measurements. On only three occasions did we double the Lomb–Scargle period to correct for a 1/2-period harmonic error, which we visually identified by noticing asymmetry in the depths of alternating minima and other subtle morphological asymmetries.

Eleven stars were observed twice, in neighboring sectors, and for these we find consistent periods across sectors. Figure 3 shows an example where we stitched the light curves from two sectors together, and found a more precise period than attained from either sector separately (based on the width of the periodogram peak). Stitching the light curves together was simplified by the fact that multiple maxima and minima were captured in each sector, which meant that no reference stars were needed to normalize the light curves from each sector.

The bottom left panels of Figures 2 and 3 plot *Gaia* DR2 color ($G_{\text{BP}} - G_{\text{RP}}$) versus P_{rot} for our sample. The majority of the stars follow a common sequence, indicating that they are coeval.

2.3. A Gyrochronological Age

Gyrochronology only requires as input the mass of a star (or a proxy like temperature or color) and its P_{rot} . There are a variety of empirical gyrochronology models available, including those of Barnes (2003), Barnes (2007) and its various re-calibrations (e.g., Mamajek & Hillenbrand 2008; Angus et al. 2015), and Barnes (2010). There are also theoretical models that pair stellar evolution with a magnetic torque law to predict angular momentum evolution (e.g., van Saders & Pinsonneault 2013; Matt et al. 2015; Gallet & Bouvier 2015). However, no model has been published that can explain all of the cluster rotation data (see Curtis et al. 2019; Douglas et al. 2019; Agüeros et al. 2018). Instead, we suggest that the best way to constrain the age of the Psc–Eri stream with gyrochronology is by comparing its P_{rot} distribution directly to the distributions measured for benchmark clusters.

2.3.1. The Benchmark Cluster Sample

The Pleiades is ≈ 120 Myr old (Stauffer et al. 1998, see also Table 1), has a metallicity of $[\text{Fe}/\text{H}] = +0.03$ dex (Soderblom et al. 2009) and an interstellar reddening of $E(B - V) \approx 0.044$ ($A_V = 0.14$; Taylor 2006). P_{rot} for 759 members were measured by Rebull et al. (2016a) from *K2* light curves collected during its Campaign 4 (see also Rebull et al. 2016b; Stauffer et al. 2016). We cross-matched this list with *Gaia* DR2 and filtered out stars that were more than 0.375 mag discrepant from the single-star sequence, which we defined with the *Gaia* Collaboration et al. (2018b) membership list; this is half of the offset for an equal-mass binary (e.g., Hodgkin

² <https://heasarc.gsfc.nasa.gov/cgi-bin/tess/webtess/wtv.py>

³ <https://mast.stsci.edu/tesscut/>

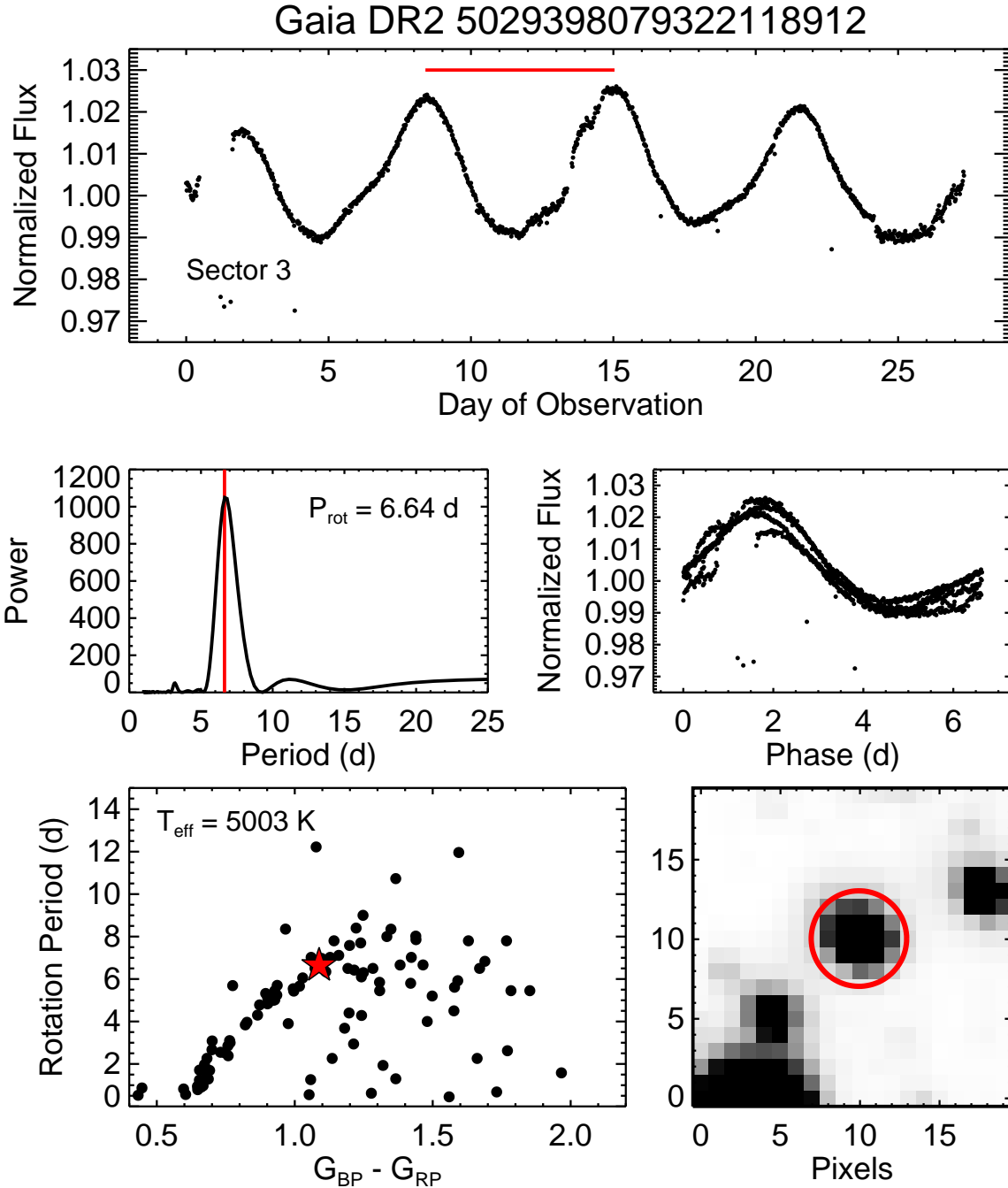


Figure 2. *Top*—Example *TESS* light curve for Gaia DR2 5029398079322118912, which was observed during Sector 3. The length of the red line at the top left is the duration of one cycle (i.e., P_{rot}). *Middle left*—The Lomb–Scargle periodogram shows $P_{\text{rot}} = 6.64 \text{ d}$. In some cases, the periodogram did not produce an accurate measurement, so we calculated P_{rot} by fitting the timing of successive maxima and/or minima, illustrated by the red line in the top panel. *Middle right*—This phase-folded light curve visually validates the periodogram analysis. *Bottom left*—The color and period for this star (red star) are plotted along with the full rotator sample for the Psc–Eri stream (black points). The *Gaia* DR2 T_{eff} is also provided (Andrae et al. 2018). *Bottom right*—The 20×20 pixel cutout of the *TESS* full frame image for this target, encircled with a three pixel radius aperture used to extract the light curve (red circle). Versions of this figure for every target analyzed are available as an electronic figure set in the online Journal (101 images).

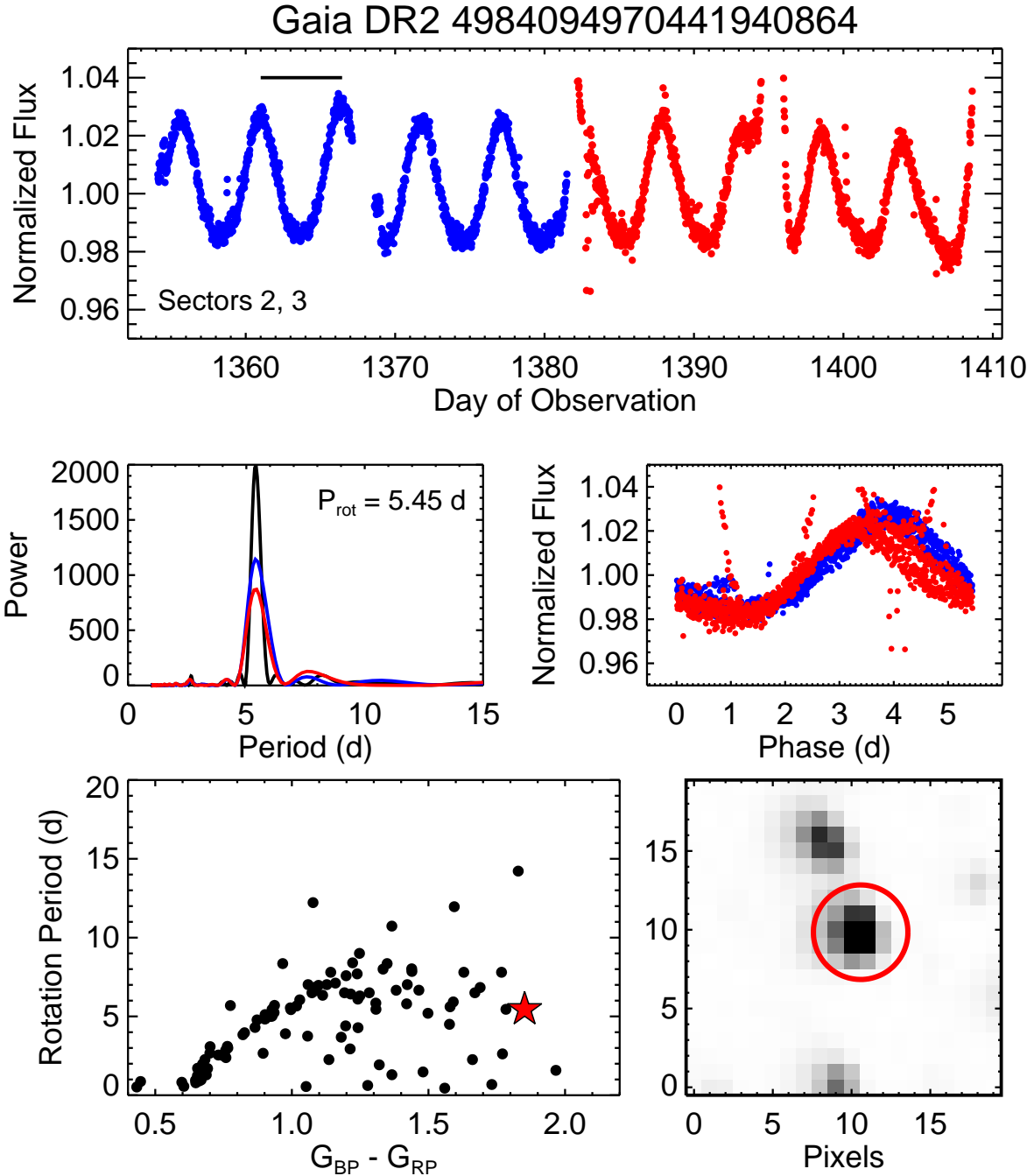


Figure 3. Similar to Figure 2, but for the 11 stars with two sectors of data. *Top*—The *TESS* light curve for Gaia DR2 4984094970441940864, which was observed during Sectors 2 (blue) and 3 (red). The length of the black line at the top left is the duration of one cycle (i.e., P_{rot}). *Middle left*—Lomb–Scargle periodograms for Sector 2 (blue), Sector 3 (red), and the joint light curve (black). While we find the same period from each individual sector, the periodogram peak is noticeably narrower for the joint light curve. *Middle right*—The phase-folded light curves for each sector show that the light curves can be reliably merged by simply stitching them together with no additional calibration needed (for these rapid, active stars, at least). *Bottom left*—The color and period for this star (red star) are plotted along with the full rotator sample for the Psc–Eri stream (black points). *Bottom right*—The 20×20 pixel cutout of the *TESS* full frame image for this target, encircled with a three pixel aperture used to extract the light curve (red circle).

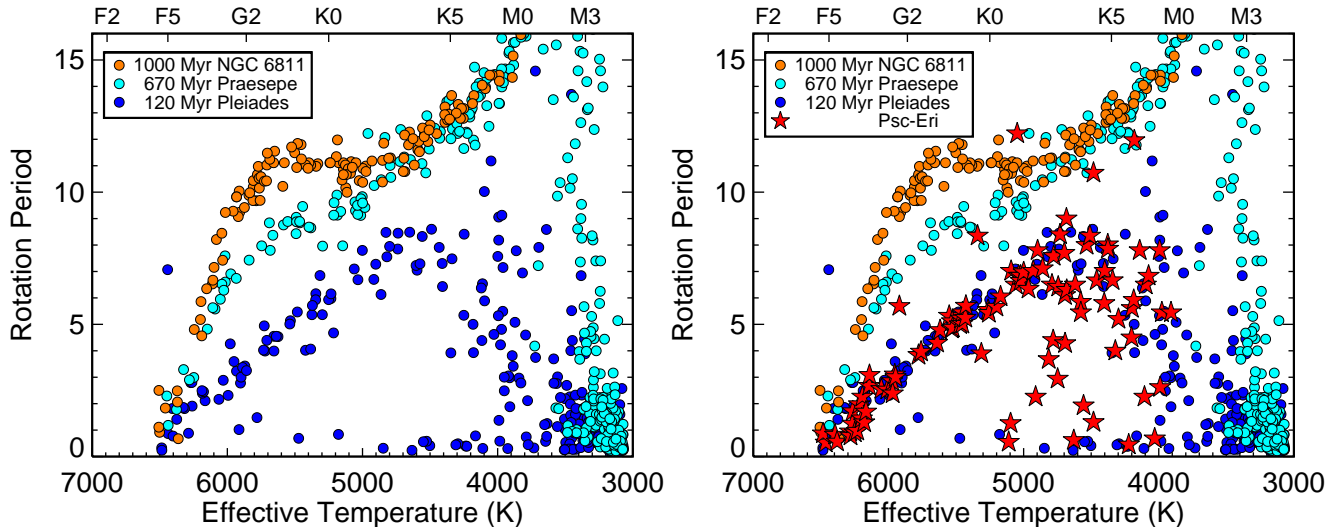


Figure 4. *Left*—Rotation period distributions for single-star members of the Pleiades (blue points, 120 Myr; [Rebull et al. 2016a](#)), Praesepe (cyan points, 670 Myr; [Douglas et al. 2017, 2019](#)), and NGC 6811 (orange points, 1 Gyr; [Curtis et al. 2019](#)). *Right*—Similar to the previous panel, and now including rotation periods for 101 members of the Psc–Eri stream (red stars) identified by [Meingast et al. \(2019\)](#), and measured by us from *TESS* FFI data. Approximate spectral types are listed at the top of each panel for reference. Clearly, the rotation period distribution for this stream favors an age much younger than 1 Gyr. We infer an age of ≈ 120 Myr for the Psc–Eri stream based on its similarity with the Pleiades.

[et al. 1999](#)). We also removed stars with absolute differences in proper motion relative to the cluster median greater than 3 mas yr^{-1} , corresponding to $\approx 2 \text{ km s}^{-1}$ at 136 pc, or four times the internal velocity dispersion ([Madsen et al. 2002](#)).

Praesepe is 670 Myr old ([Douglas et al. 2019](#)) and has a metallicity of $[\text{Fe}/\text{H}] = +0.15$ dex ([Cummings et al. 2017](#)). P_{rot} for 743 members were amassed from the literature and measured from *K2* Campaign 5 light curves by [Douglas et al. \(2017\)](#). [Douglas et al. \(2019\)](#) cross-matched this list with DR2 and filtered out stars that failed membership, multiplicity, and data quality criteria, leaving us with 359 single star members.

The 1 Gyr-old NGC 6811 cluster has a solar metallicity ([Sandquist et al. 2016](#)). P_{rot} for 171 likely single-star members were recently measured by [Curtis et al. \(2019\)](#), more than doubling the size of the rotator sample from [Meibom et al. \(2011b\)](#), and extending its lower mass limit from $\approx 0.8 M_{\odot}$ to $\approx 0.6 M_{\odot}$.

2.3.2. Stellar Properties

Gaia DR2 provided effective temperatures (T_{eff}) for $\approx 1.61 \times 10^8$ stars with $3000 \lesssim T_{\text{eff}} \lesssim 10,000$ K and $G < 17$ mag ([Gaia Collaboration et al. 2018b](#)) via the Apsis pipeline ([Bailer-Jones et al. 2013](#)). The DR2 photometry is very precise, but the Apsis temperatures are severely affected by interstellar reddening. However, this bias can be mitigated by de-reddening the photometry for each cluster sample prior to converting it

to T_{eff} . We employ an empirical color–temperature relation to convert the de-reddened *Gaia* DR2 ($G_{\text{BP}} - G_{\text{RP}}$)₀ color to T_{eff} . Our relation is a polynomial fit to benchmark stellar data assembled from the catalog of spectroscopic properties for the solar-type stars ($4700 < T_{\text{eff}} < 6700$ K) targeted by the California Planet Survey ([Brewer et al. 2016](#)), warmer stars taken from the Hyades ([Gaia Collaboration et al. 2018b](#)) with T_{eff} from the DR2/Apsis pipeline ([Andrae et al. 2018](#)), and cooler K and M dwarfs from the [Boyajian et al. \(2012\)](#) and [Mann et al. \(2015\)](#) catalogs. We have also applied this relation in [Morris et al. \(2018\)](#), [Douglas et al. \(2019\)](#), and [Curtis et al. \(2019\)](#).

2.3.3. The Psc–Eri Stream is Coeval with the Pleiades

In the left panel of Figure 4, we present the P_{rot} distribution for likely single-star members of our three benchmark open clusters as a function of T_{eff} . In the right panel, we add the the P_{rot} distribution for the Psc–Eri stream. The Psc–Eri stream’s P_{rot} distribution is nearly indistinguishable from that of the Pleiades. In particular, the slow, converged sequences for each system are remarkably consistent.

There are a few differences. The Psc–Eri stream has more outliers at periods intermediate to the slow sequence and the rapid ≈ 1 d rotators. This could be due to poor binary rejection, or slight differences in age—if younger than the Pleiades, those stars could still be converging. In addition, the Pleiades sample extends

to much cooler T_{eff} . As we discuss in Section 3.1, this is because RVs were used to identify members of the Psc–Eri stream, and DR2 does not provide RVs for such cool and faint stars. Finally, the warmest stars in the Psc–Eri stream ($T_{\text{eff}} \gtrsim 6100$ K) appear to be rotating subtly and systematically faster than their analogs in the Pleiades. Perhaps this also indicates that the stream is slightly younger than the Pleiades.

In contrast, the late-F to early-K dwarfs are, again, remarkably consistent. The slow, converged sequences for both populations are well-described by a line of constant Rossby number.⁴ Focusing on the stars with $4600 < T_{\text{eff}} < 6100$ K that have converged to within 25% of the slow sequence, the median and standard deviation of the Rossby number for the 43 Pleiades in this sample is $Ro = 0.29 \pm 0.03$, and we find $Ro = 0.29 \pm 0.02$ for the 39 stream members meeting the same criteria. These values are incredibly precise, and strikingly similar. The unavoidable conclusion is that the Psc–Eri stream is ≈ 120 Myr in age.⁵

3. REVISITING THE PSC–ERI STREAM’S CMD

The left panel of Figure 5 is the CMD for the stream,⁶ together with members of the Pleiades (Gaia Collaboration et al. 2018b) and NGC 6811 Curtis et al. (2019). We also include PARSEC isochrones (Bressan et al. 2012) appropriate for the Pleiades (130 Myr, solar metallicity), and NGC 6811 (1 Gyr, solar metallicity).

3.1. The Apparent Absence of a Main-Sequence Turnoff Is a Problem

The absence of Psc–Eri members warmer than $T_{\text{eff}} \approx 7760$ K on the main sequence would seem to favor an older age for the stream. However, as Meingast et al. (2019) pointed out, the stream lacks a clear main-sequence turnoff (MSTO). This is a problem: if the Psc–Eri stream is 1 Gyr old, there should be a well-defined MSTO (Figure 5 shows the case of NGC 6811). If the stream is young, the higher-mass stars should fol-

low the Pleiades main sequence. Either way, these stars should exist somewhere in the CMD, but they are either missing from the stream or missing from its membership catalog.

Identifying members of most star clusters is facilitated by their spatial overdensity and distance from Earth: proper motion are sufficient, and RVs are not strictly needed for finding candidate members. Identifying members of moving groups, stellar streams, and very nearby clusters (e.g., the Hyades) is more difficult because 3D kinematics are required. Accordingly, Meingast et al. (2019) used RVs to identify candidate Psc–Eri stream members. But the Gaia Radial Velocity Spectrometer (Soubiran et al. 2013; Cropper et al. 2018) provided measurements for stars with $3550 \lesssim T_{\text{eff}} \lesssim 6900$ K (Katz et al. 2018) in DR2. This data limitation means that the Meingast et al. (2019) criteria automatically precluded the identification of the MSTO for the Psc–Eri stream.

The left panel of Figure 5 plots the Pleiades membership (Gaia Collaboration et al. 2018b), and highlights those with DR2 RVs. The CMD for this Pleiades RV sample looks identical to the Meingast et al. (2019) membership for the Psc–Eri stream. We conclude that selecting members while requiring Gaia RVs will exclude warmer members, if they exist (as well as the coolest, lowest-mass stars and hot white dwarfs).

3.2. New, Massive Candidate Psc–Eri Members Support a Young Age

If the Psc–Eri stream is the same age as the Pleiades, we should be able to identify hotter, more massive stars that are spatially and kinematically consistent with the Meingast et al. (2019) members. To this end, we queried DR2 for stars with $G < 10$ mag, $(G_{\text{BP}} - G_{\text{RP}}) < 0.5$, and $M_G < 3$ mag, which returned 435,601 stars. We trimmed this to 6851 stars by selecting those consistent with the stream in R.A. versus $\mu_\alpha \cos \delta$, R.A. versus π , and decl. versus μ_δ diagrams. Next, we searched SIMBAD (Wenger et al. 2000) for RV measurements for these stars. We found 2332 matches for which we could then calculate 3D galactic UVW velocities.

Of these, 22 are within 5 km s^{-1} of the median value of the Meingast et al. (2019) members and within 20 pc of at least one member.⁷ While our velocity criterion is less restrictive than the 1.3 km s^{-1} velocity dispersion found by Meingast et al. (2019), our larger threshold is

⁴ $Ro = P_{\text{rot}}/\tau$. We used the formula for convective turnover time, τ , from Cranmer & Saar (2011).

⁵ We performed similar comparisons with M35 (NGC 2168, 150 Myr; Meibom et al. 2009) and M34 (NGC 1039, 220 Myr; Meibom et al. 2011a), and found that the Psc–Eri P_{rot} distribution was most consistent with that of the Pleiades. Specifically, the slow sequences for the older M35 and M34 clusters are converged to lower masses and longer periods (see figure 12 in Stauffer et al. 2016), whereas the slow sequences for Psc–Eri and the Pleiades share a common maximum P_{rot} of ≈ 8.5 d, where the distributions turn over toward more rapid rotation toward lower masses and cooler temperatures.

⁶ We adopt $d = 1000/\varpi$ to estimate distances for each star, and so calculate absolute magnitudes as $M_G = G - 5 \log_{10}(100/\varpi)$, with units of pc and mas for d and ϖ .

⁷ The median and maximum separation between nearest neighbors in the Meingast et al. (2019) membership list is 9 and 26 pc; the median and maximum velocity deviations from the stream’s average UVW velocity are 3 and 6 km s^{-1} .

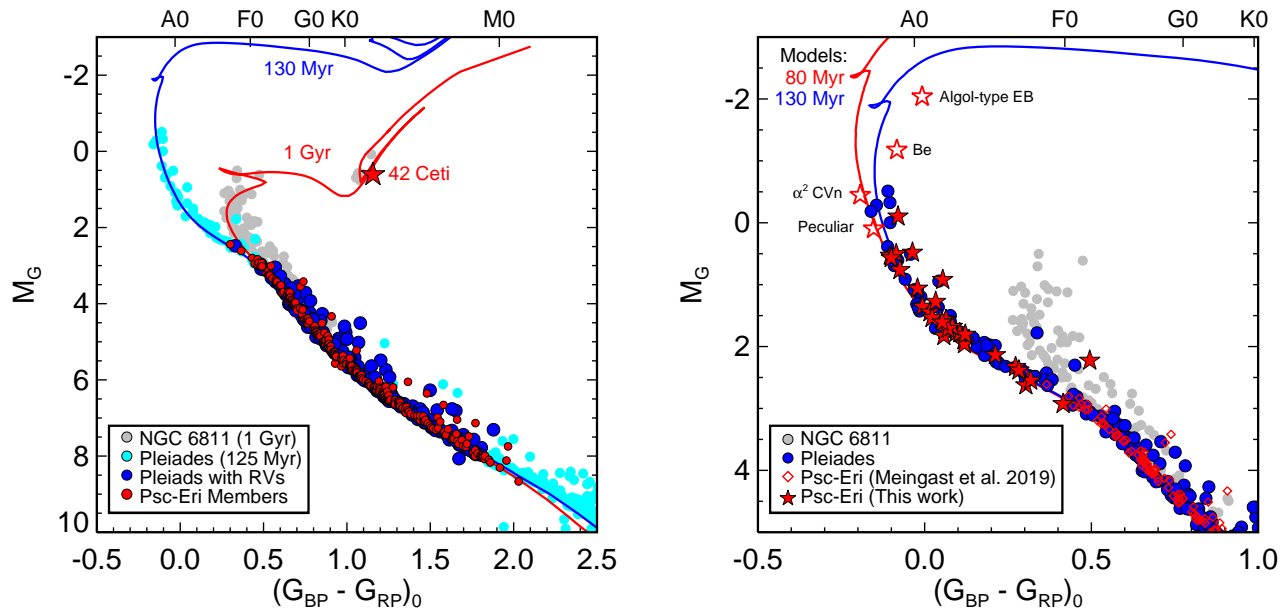


Figure 5. *left*—De-reddened *Gaia* DR2 color versus absolute magnitude for NGC 6811 (gray points; $(m-M) = 10.2$, $A_V = 0.15$; Curtis et al. 2019), the stream (red points; distance moduli are calculated directly from parallax, zero reddening is assumed Meingast et al. 2019), the Pleiades (cyan points; $(m-M) = 5.67$, $A_V = 0.14$; Gaia Collaboration et al. 2018b), and the subset of Pleiades with DR2 RVs (blue points). PARSEC isochrones with solar metallicity are overlaid in blue (130 Myr) and red (1 Gyr). The Pleiades sub-sample with RVs covers a nearly identical range in color and absolute magnitude as the stream’s published membership. This demonstrates that the stream’s apparent turnoff color, which otherwise appears similar to NGC 6811’s, is biased by the lack of RV coverage in DR2 for warmer stars. The sole evolved member of the stream is 42 Ceti, which has an isochrone age of ≈ 1 Gyr; this is at odds with our gyrochronology age and suggests that it is an interloper. *Right*—We identified 34 stars (red stars) that are warmer than the Meingast et al. (2019) list (red open diamonds), and which closely track the Pleiades upper main sequence (blue points). Twenty two were found by pairing DR2 astrometry with literature RVs to determine their 3D kinematics, and the remaining twelve are co-moving neighbors in proper motion of Meingast et al. (2019) members. Four of these candidates (red open stars) have peculiar abundances or are expected to have atypical photometry (open stars); disregarding them, our high-mass candidates closely track the Pleiades upper main sequence.

justified by the fact that hotter, rapidly rotating stars will have less precise RVs than those for the FGK dwarfs reported in DR2.⁸

We also searched the 10 pc volume around every Meingast et al. (2019) member for co-moving neighbors, according to the proper motion criterion $\Delta\mu < 2$ mas yr⁻¹, and found 377 co-moving candidates, including ten high-mass stars. Oh et al. (2017) performed a similar exercise to identify co-moving pairs and larger groups using a more sophisticated algorithm applied to the *Tycho-Gaia* Astrometric Solution (TGAS; Michalik et al. 2015) catalog, released with *Gaia* DR1 (see also Andrews et al. 2017). While the Psc-Eri stream was not identified as a co-moving system in their analysis, they did identify seven high-mass stars as co-moving part-

ners with members from Meingast et al. (2019), adding two unique stars to our high-mass candidate list (12 co-moving neighbors in total). Table 4 lists our 34 high-mass candidate members.

The right panel of Figure 5 shows the CMD for the Pleiades members together with the Meingast et al. (2019) Psc-Eri stream members and our high-mass candidate members. The Pleiades has 239 members with DR2 RVs (Gaia Collaboration et al. 2018b), and Meingast et al. (2019) identified 256 members of the Psc-Eri stream. The sizes of these samples are approximately equal, so we expect that the Psc-Eri stream should have a similar number of higher-mass stars, and perhaps a similar population size and total mass.⁹ The Pleiades

⁸ Restricting the velocity criterion to ≤ 3 km s⁻¹ reduces the candidate list from 22 to 11 stars. Similarly, only 55% of the Meingast et al. (2019) list has $\Delta v \leq 3$ km s⁻¹ in Cartesian *UVW* velocities.

⁹ For reference, the Pleiades has over 1000 known members: Gaia Collaboration et al. (2018b) identified 1332 members and Cantat-Gaudin et al. (2018) identified 1061 members with *Gaia* DR2 (see also Sarro et al. 2014). Adams et al. (2001) estimated a total mass of $\approx 800 M_\odot$.

list has 43 more that are brighter and warmer than $T_{\text{eff}} \approx 7000$ K RV cutoff, and we found 34 candidates in the stream.

Two of the five brightest candidates in the CMD are expected to have atypical photometry and should be excluded from an isochronal age analysis (Cummings & Kalirai 2018): according to SIMBAD, λ Tau is an Algol-type eclipsing binary and omi Aqr is a Be star. Focusing on the blue edge of the upper main sequence, the Psc–Eri stream appears approximately coeval with the Pleiades. The 80 Myr and 130 Myr PARSEC isochrones shown in the right panel of Figure 5 do not diverge appreciably in color at the luminosities covered by the Pleiades and Psc–Eri stream samples. We postpone a precise isochronal analysis until we can validate the membership of our high-mass candidates with new RV measurements.

3.3. How Did the Psc–Eri Stream Form?

Meingast et al. (2019) estimated the Psc–Eri stream progenitor cluster mass to be $\approx 2000 M_{\odot}$, noted that the Hyades initial mass has been estimated to be $\approx 1700 M_{\odot}$, and concluded that since the Hyades still has a gravitationally bound core, the Psc–Eri stream, which has been dispersed, must be older.

Indeed, if it were truly 1 Gyr old, the Psc–Eri stream would have had to be born as a dense cluster analogous to the Pleiades, Hyades, or NGC 6811, to survive for so long before disrupting. However, given that we now know that it is actually ≈ 120 Myr, this constraint on the stream’s birth conditions is unnecessary. In their figure A.1 and table A.2, Meingast et al. (2019) identified four main clumps within the stream. These clumps are presently separated by ≈ 160 pc, and this clumpiness is similar to that seen in the much younger Tuc–Hor (Kraus et al. 2014) or Sco–Cen associations (Preibisch & Mamajek 2008; Pecaut & Mamajek 2016; Wright & Mamajek 2018), which are gravitationally unbound.

We suggest that the members of the Psc–Eri stream were not formed in a dense cluster but instead formed in a more decentralized fashion, similar to these OB associations. If correct, this would resolve two challenges to our young age result:

1. *Why does the stream not have a well defined core?*
Our answer is that it never had one, but instead formed several smaller clumps.
2. *How could a 120-Myr-old cluster disperse its stars across 400 pc with such a low internal velocity dispersion?* The ends of stream had a head start, as they were born separated in space, and the members of each subgroup dispersed from there.

According to the Gaia Collaboration et al. (2018b) membership lists, the Pleiades has 611 members within 5 pc of its center, and the Hyades has 195 members in the same size volume. In contrast, we suggest that the stream formed multiple approximately coeval clumps; therefore, each zero-age core density is much less than expected based on the present-day star count.

If we are correct, this would mean that the stream provides an environment to its stars that is distinct from that of the Pleiades, and which might be representative of a more common star formation channel in the Galaxy than dense cluster formation (e.g., Clark et al. 2005). That would make the Psc–Eri stream an excellent target for exoplanet searches, which have so far turned up nothing for the Pleiades (Gaidos et al. 2017).

4. CONCLUSION

Meingast et al. (2019) discovered an exciting new stellar stream located relatively nearby ($d \simeq 80$ –226 pc). We were intrigued by its apparently old age (≈ 1 Gyr), as this would make it a critical target for the calibration and validation of a variety of age-dating techniques, including stellar activity, rotation, lithium depletion, and other chemical clock techniques.

Using new time series photometry from *TESS*, we measured P_{rot} for 101 of the Psc–Eri stream’s members. We found that the majority of these members actually overlap with the P_{rot} distribution for the Pleiades, indicating that the Psc–Eri stream is only ≈ 120 Myr old.

By contrast to the CMD for the ≈ 1 Gyr old cluster NGC 6811, the Meingast et al. (2019) CMD for the Psc–Eri stream lacked a MSTO. We concluded that this is because the Psc–Eri stream is young, and that the more massive stars that would otherwise occupy the MSTO are warmer than the $T_{\text{eff}} \lesssim 7000$ K cutoff for the *Gaia* DR2 RV dataset; i.e., warmer stars could not be detected in DR2 as members by Meingast et al. (2019) because they lack 3D kinematics. We expanded the search for these missing members by pairing DR2 with RV measurements in the literature tabulated by SIMBAD, and also by searching for co-moving neighbors to the known members. We found 34 candidates that closely track the upper main sequence of the Pleiades, further strengthening our finding of a young age for the Psc–Eri stream.

There is one point on the Psc–Eri stream’s CMD consistent with an old age: the evolved 42 Cet triple system. Given the indisputably young age for the Psc–Eri stream we found with gyrochronology, we suspect it is an interloper.

Meingast et al. (2019) estimated that the stream was formed with a total stellar mass similar to the Hyades. The Hyades has retained a dense cluster structure (with

tidal tails; Meingast & Alves 2019), as has the Pleiades, while the stream is diffuse, with an elongated structure spanning 400 pc with four clumps. We argued that rather than being evidence for an older age, this structure indicates that the Psc–Eri stream’s stars did not form in a dense cluster environment, but instead in the more decentralized fashion typical of OB associations.

If true, the Psc–Eri stream could become a valuable benchmark system for comparing environmental impact relative to the Pleiades, and for examining how photo-evaporation sculpts planet sizes. To date, no planets have been found in the Pleiades (Gaidos et al. 2017). The stream thus presents a new opportunity to search for Pleiades-aged planets. Indeed, a Psc–Eri member

has already been identified as a planet candidate host with *TESS*.¹⁰

This is the first gyrochronology study using *TESS* data, and it confirms that *TESS* will be an exciting mission for stellar astrophysics. This is especially true given how *TESS* records and releases FFI data. The existence of this stream was not known prior to the *TESS* Cycle 1 call for proposals, and yet the FFI data were ready for us to analyze immediately following the announcement of the stream’s discovery by Meingast et al. (2019). This is also the first time a stellar stream has been age-dated using gyrochronology, and our work demonstrates the potential for gyrochronology to serve as a powerful tool for Galactic archaeology.

Table 2. Rotation periods for Meingast et al. (2019) members of the Psc–Eri stream

#	<i>Gaia</i> DR2 Source ID	R.A.	decl.	($G_{BP} - G_{RP}$)	G	M_G	P_{rot}	Notes
		[h:m:s]	[d:m:s]	[mag]	[mag]	[mag]	[d]	
1	3198972700981234048	04:22:31.5	−07:33:03.2	0.432	8.903	2.802	0.52	Warm
2	5181474045115843072	03:10:47.3	−06:34:29.8	0.446	8.562	2.954	0.87	Warm
3	2516948215250061568	02:20:22.6	+05:52:59.1	0.597	9.183	3.534	0.82	Warm
4	3245408684793798528	04:02:15.4	−05:53:48.2	0.604	9.425	3.513	0.56	Conv.
5	6628071944405827712	22:36:31.1	−21:35:06.0	0.647	8.967	3.835	0.94	Conv.
6	2988966044497883392	05:22:51.9	−11:47:47.8	0.648	10.345	3.688	0.79	Conv.
7	2456987757379368064	01:32:34.4	−12:51:09.7	0.654	9.043	3.865	1.24	Conv.
8	3186195241994234880	04:43:02.6	−07:53:54.6	0.655	9.999	3.766	1.71	Conv.
9	2988096919213031808	05:02:35.2	−12:31:20.4	0.661	10.280	3.869	0.91	Conv.
10	2987729922847457280	05:07:09.2	−13:34:07.7	0.668	10.156	3.896	0.97	Conv.
11	3204844780267292288	04:29:21.6	−02:49:47.1	0.673	9.760	4.020	1.98	Conv.
12	2405544971274027904	23:21:22.3	−17:30:58.5	0.680	9.222	4.024	1.44	Conv.
13	3190206672727634816	04:01:28.8	−11:19:25.7	0.682	9.920	4.059	2.26	Conv.
14	5182223980765557248	03:18:22.8	−04:29:29.0	0.687	9.788	4.054	1.29	Conv.
15	2982998926174605824	05:10:30.1	−16:08:04.1	0.691	10.646	3.970	1.70	Conv.
16	2492898356897645184	02:18:04.2	−03:50:14.4	0.700	9.453	4.126	2.67	Conv.
17	3256702490277205376	04:03:24.9	−00:46:45.2	0.701	9.928	4.180	3.08	Conv.
18	5104477754084350464	03:15:18.8	−17:56:36.4	0.731	9.606	4.279	2.55	Conv.
19	5147686052794315904	02:02:10.9	−16:34:03.4	0.746	9.643	4.410	2.53	Conv.
20	3197608241410937216	04:32:01.8	−08:53:13.7	0.758	10.494	4.476	2.85	Conv.

Table 2 continued

¹⁰ First noted by Elisabeth Newton as a Psc–Eri member (priv. comm.), TOI 451 is a G dwarf with $T_{eff} \approx 5530$ K (*Gaia* DR2 4844691297067063424, CD–38 1467, TIC 257605131). Our analysis of the *TESS* 2 min light curves from Sectors 4 and 5 reveals two sets of transits, suggesting that TOI 451 hosts two planets with $P_{orb,b} \approx 9.19$ d and $P_{orb,c} \approx 16.36$ d. Follow-up efforts to rule out false positive scenarios and validate the planetary system are being coordinated by the *TESS* Hunt for Young Moving group Exoplanets collaboration (THYME).

Table 2 (continued)

#	<i>Gaia</i> DR2 Source ID	R.A.	decl.	$(G_{\text{BP}} - G_{\text{RP}})$	G	M_G	P_{rot}	Notes
		[h:m:s]	[d:m:s]	[mag]	[mag]	[mag]	[d]	
21	2489889607752127360	02:18:43.9	-04:00:56.0	0.759	10.019	4.390	2.39	Conv.
22	2346216668164370432	00:54:13.5	-22:53:07.8	0.764	9.441	4.452	3.10	Conv.
23	5129126330877050240	02:46:34.6	-18:54:17.5	0.766	9.784	4.520	3.00	Conv.
24	5070969209513725568	02:38:36.5	-25:15:07.6	0.775	9.435	4.462	5.69	Slow
25	2493286445846897664	02:15:46.4	-02:36:32.5	0.821	9.916	4.813	3.84	Conv.
26	3197753548744455168	04:33:55.4	-08:19:27.9	0.827	10.892	4.799	3.96	Conv.
27	2513568007268649728	02:14:47.2	+02:14:20.4	0.865	10.473	5.025	4.30	Conv.
28	5179904664065847040	03:09:03.7	-07:03:55.8	0.873	10.382	4.979	4.78	Conv.
29	5168681021169216896	03:29:30.3	-07:10:13.8	0.895	10.827	5.204	5.32	Conv.
30	3253302456727341696	04:07:34.7	-02:04:33.2	0.901	10.982	5.112	4.83	Conv.
31	3176016268285396864	04:21:35.2	-14:01:29.9	0.902	11.335	5.263	5.11	Conv.
32	2531732317316926336	01:15:31.7	-02:50:46.4	0.903	10.841	5.210	4.87	Conv.
33	2495781619982992640	02:45:01.2	-02:25:46.3	0.921	10.780	5.304	5.00	Conv.
34	2968825259219765120	05:29:28.5	-19:17:58.8	0.924	12.032	5.264	5.22	Conv.
35 ^a	4844691297067063424	04:11:51.9	-37:56:23.03	0.927	10.750	5.280	5.02	Conv.
36	2496200774431287424	02:30:58.8	-03:03:04.9	0.928	10.415	5.328	5.45	Conv.
37	4980826504625538048	00:38:12.2	-43:00:24.8	0.935	10.317	5.401	5.24	Conv.
38	4842810376267950464	03:47:56.3	-41:56:24.9	0.936	10.762	5.383	5.70	Conv.
39	3198734278756825856	04:26:27.1	-07:39:39.7	0.966	11.469	5.445	8.35	Slow
40	5045955865443216640	03:00:46.9	-37:08:01.5	0.976	10.323	5.363	3.90	Rapid
41	3193528950192619648	03:57:04.0	-10:14:00.9	0.994	11.297	5.534	5.54	Conv.
42	3187547465200970368	04:46:12.3	-07:32:24.4	0.997	11.733	5.519	5.43	Conv.
43	3245140743257978496	03:54:01.0	-06:14:14.6	1.017	11.146	5.434	5.66	Conv.
44	3205573756476323328	04:23:54.6	-02:33:43.4	1.029	11.604	5.634	6.05	Conv.
45	3185678437170300800	04:34:42.8	-08:57:18.5	1.052	11.899	5.796	0.55	Rapid
46	5103353606523787008	03:18:03.8	-19:44:14.2	1.058	10.473	5.227	1.26	Rapid
47	3187477818011309568	04:47:58.2	-07:49:25.2	1.059	11.994	5.818	7.02	Conv.
48	3009905594911137664	05:26:30.0	-12:01:21.1	1.073	12.576	5.905	6.50	Conv.
49	5083255496041631616	03:57:35.1	-24:28:42.2	1.077	11.131	5.885	12.22	Slow
50	3243665031151732864	03:48:38.3	-06:41:52.6	1.082	11.460	5.953	6.84	Conv.
51	3192643431015406464	04:21:53.2	-08:43:16.1	1.088	11.752	5.873	6.84	Conv.
52	5029398079322118912	01:13:42.4	-31:11:39.6	1.088	10.804	5.959	6.64	Conv.
53	2596395760081700608	22:39:53.5	-16:36:23.3	1.097	11.508	5.994	6.97	Conv.
54	2979827384884386176	04:58:02.5	-17:10:27.7	1.113	12.317	6.033	6.34	Conv.
55	3196687812738993152	04:06:00.2	-06:53:50.0	1.128	11.842	6.073	7.02	Conv.
56	2491594263092190464	02:10:22.3	-03:50:56.7	1.136	11.533	6.153	2.26	Rapid
57	2402197409339616768	22:39:01.4	-18:52:55.7	1.142	11.219	6.155	7.80	Conv.
58	3013355999838366336	05:25:14.6	-10:25:49.4	1.159	12.806	6.185	7.11	Conv.
59	5096891158212909312	04:12:46.0	-16:19:29.1	1.181	11.994	6.187	3.68	Rapid
60	4871041608622321664	04:28:28.9	-33:53:45.1	1.193	11.630	6.037	6.50	Rapid

Table 2 continued

Table 2 (continued)

#	<i>Gaia</i> DR2 Source ID	R.A.	decl.	$(G_{\text{BP}} - G_{\text{RP}})$	G	M_G	P_{rot}	Notes
		[h:m:s]	[d:m:s]	[mag]	[mag]	[mag]	[d]	
61	7324465427953664	03:05:14.1	+06:08:53.5	1.197	12.043	6.247	4.40	Rapid
62	5097262136011410944	03:58:54.7	-17:05:53.2	1.199	11.649	6.311	7.58	Conv.
63	2418664520110763520	23:49:55.1	-15:43:42.0	1.213	11.607	6.396	2.94	Rapid
64	5179037454333642240	02:39:10.9	-05:32:22.5	1.215	11.765	6.373	6.42	Rapid
65	2484875735945832704	01:24:24.7	-03:16:39.0	1.222	11.791	6.398	8.40	Conv.
66	2393862836322877952	23:40:37.5	-18:11:37.9	1.239	11.485	6.472	7.70	Conv.
67	2594993646533642496	22:31:13.9	-17:04:52.4	1.242	11.934	6.451	6.10	Rapid
68	3199896668704440064	04:38:55.5	-06:40:25.0	1.242	12.458	6.305	4.28	Rapid
69	5114686272872474880	03:47:25.8	-12:32:30.9	1.247	12.634	6.550	9.00	Conv.
70	2433715455609798784	23:36:52.1	-11:25:01.7	1.249	11.737	6.442	6.30	Rapid
71	5106733402188456320	03:24:25.2	-15:50:05.4	1.278	11.517	6.197	0.62	Rapid
72	2390974419276875776	23:48:32.4	-18:32:57.4	1.283	11.583	6.618	6.50	Rapid
73	3172630287868034944	04:26:48.2	-15:25:47.4	1.307	12.334	6.599	5.85	LM
74	5161117923061794688	02:59:52.0	-09:47:35.8	1.308	12.063	6.639	5.45	LM
75	5155187986271622912	03:20:33.3	-14:16:58.4	1.320	12.307	6.687	1.93	LM
76	5129876953722430208	02:29:28.5	-20:12:16.8	1.334	11.695	6.739	8.00	LM
77	2339984636258635136	23:56:53.7	-23:17:24.6	1.349	11.475	6.765	8.35	LM
78	3195826963854173056	04:06:29.4	-07:35:32.2	1.366	12.987	6.797	10.73	Slow
79	2349094158814399104	00:47:18.0	-22:45:08.1	1.366	10.929	6.051	1.30	LM
80	3247412647814482816	03:32:30.9	-06:13:09.1	1.382	12.327	6.898	6.66	LM
81	4975223840046231424	00:47:38.5	-47:41:45.8	1.420	11.514	6.985	5.80	LM
82	3191365111308746880	04:24:30.4	-10:41:02.4	1.423	12.901	6.944	7.02	LM
83	3197607794734344320	04:31:51.6	-08:54:03.5	1.439	13.133	7.059	8.02	LM
84	3171136944919260928	04:36:36.1	-17:47:23.7	1.439	12.879	6.940	7.85	LM
85	3206907086126334464	05:13:25.5	-08:19:52.2	1.465	13.320	7.086	6.66	LM
86	3177883999240571904	04:35:35.3	-12:47:47.6	1.480	12.828	6.356	4.00	LM
87	2488721720245150336	02:26:53.3	-05:17:45.2	1.498	12.485	7.198	5.20	LM
88	5159567164990031360	03:04:46.0	-12:16:57.9	1.560	12.613	7.098	0.45	LM
89	5081912751826042624	03:47:01.6	-26:16:11.2	1.577	12.968	7.389	4.50	LM
90	5118895478259982336	02:26:07.0	-24:54:49.0	1.579	11.728	6.658	5.61	LM
91	5117016378528360448	02:17:14.6	-27:16:41.9	1.591	12.551	7.451	5.92	LM
92	5149427640557882368	02:02:58.3	-13:37:46.8	1.594	11.982	7.442	11.96	Slow
93	4832163770817481856	03:58:17.4	-46:34:13.0	1.630	12.992	7.559	7.80	LM
94	2531488844210764544	01:08:57.0	-03:01:32.0	1.661	13.074	7.612	2.26	LM
95	2480756793589426944	01:33:49.3	-04:28:41.7	1.670	13.216	7.682	6.50	LM
96	2355466790769878400	00:55:21.5	-21:24:03.7	1.689	12.341	7.578	6.84	LM
97	5114516020369038848	03:51:15.9	-12:23:46.4	1.732	13.375	7.484	0.68	LM
98	5068272932125221504	02:26:04.6	-29:23:48.9	1.768	12.815	8.000	7.80	LM
99	5094664333632217088	04:02:18.0	-18:42:45.4	1.771	12.631	7.134	2.62	LM
100	5121805541941481472	01:57:17.2	-25:13:49.6	1.784	12.793	7.931	5.45	LM

Table 2 continued

Table 2 (continued)

#	<i>Gaia</i> DR2 Source ID	R.A.	decl.	$(G_{\text{BP}} - G_{\text{RP}})$	G	M_G	P_{Tot}	Notes
		[h:m:s]	[d:m:s]	[mag]	[mag]	[mag]	[d]	
101	4984094970441940864	01:21:49.7	-42:01:22.3	1.852	12.731	8.099	5.45	LM

NOTE—Columns: # is the row number sorted by $(G_{\text{BP}} - G_{\text{RP}})$; R.A., decl., $(G_{\text{BP}} - G_{\text{RP}})$, G , and $M_G = G - 5 \log_{10}(100/\pi)$ are from *Gaia* DR2; P_{Tot} is measured from *TESS* FFI data (days). The notes indicate if a star is converged on the slow sequence (“Conv.”), slower than the converged sequence (“Slow”), more rapid than the converged sequence (“Rapid”), has a lower mass (“LM”) than the converged sequence limit, or is too warm to efficiently spin down (“Warm”). notes on particular stars. Six stars appear to rotate more slowly than the bulk of the sample. Blending is not a concern for these stars (i.e., none have bright neighbors in DR2 within 1’5), their spot-modulated light curves show unambiguous periodicity, and they do not appear to be binaries according to their photometry, RV errors ($\sigma < 2 \text{ km s}^{-1}$), and kinematics. It is unclear to us why they are outliers.

^aThis star has been identified as a planet candidate host by *TESS* (TOI 451, TIC 257605131), and appears to show two sets of transits with periods of 9.19 d and 16.36 d, which await validation.

We thank Stefan Meingast for kindly providing us with the Meingast et al. (2019) membership list prior to its posting to the CDS, and Tim White for helpful discussions about 42 Ceti. The association of TOI 451 with Psc–Eri was first noted by Elisabeth Newton; we thank her and the THYME collaboration, including Aaron Rizzuto, Andrew Vanderburg, Andrew Mann, and Benjamin Tofflemire, and Adam Kraus for discussing this exciting planet candidate with us.

J.L.C. is supported by the National Science Foundation Astronomy and Astrophysics Postdoctoral Fellowship under award AST-1602662.

Part of this research was carried out at the Jet Propulsion Laboratory, California Institute of Technology, under a contract with NASA.

The Center for Exoplanets and Habitable Worlds is supported by the Pennsylvania State University, the

Eberly College of Science, and the Pennsylvania Space Grant Consortium.

This work has made use of data from the European Space Agency (ESA) mission *Gaia*,¹¹ processed by the *Gaia* Data Processing and Analysis Consortium (DPAC).¹² Funding for the DPAC has been provided by national institutions, in particular the institutions participating in the *Gaia* Multilateral Agreement.

This research made use of NASA’s Astrophysics Data System, and the VizieR and SIMBAD (Wenger et al. 2000) databases, operated at CDS, Strasbourg, France.

Facilities: *TESS*, *Gaia*

Software: TheIDL Astronomy User’s Library (Landsman 1993)¹³, TESScut (i.e., Astrocut; Brasseur et al. 2019)¹⁴

REFERENCES

- Adams, J. D., Stauffer, J. R., Monet, D. G., Skrutskie, M. F., & Beichman, C. A. 2001, *AJ*, 121, 2053
- Agüeros, M. A., Bowsher, E. C., Bochanski, J. J., et al. 2018, *ApJ*, 862, 33
- Andrae, R., Fouesneau, M., Creevey, O., et al. 2018, *A&A*, 616, A8
- Andrews, J. J., Chanamé, J., & Agüeros, M. A. 2017, *MNRAS*, 472, 675
- Angus, R., Aigrain, S., Foreman-Mackey, D., & McQuillan, A. 2015, *MNRAS*, 450, 1787
- Bailer-Jones, C. A. L., Andrae, R., Arcay, B., et al. 2013, *A&A*, 559, A74
- Baraffe, I., Homeier, D., Allard, F., & Chabrier, G. 2015, *A&A*, 577, A42
- Barnes, S. A. 2003, *ApJ*, 586, 464
- . 2007, *ApJ*, 669, 1167
- . 2010, *ApJ*, 722, 222
- Boyajian, T. S., von Braun, K., van Belle, G., et al. 2012, *ApJ*, 757, 112

¹¹ <https://www.cosmos.esa.int/gaia>

¹² <https://www.cosmos.esa.int/web/gaia/dpac/consortium>

¹³ <https://github.com/wlandsman/IDLAstro>

¹⁴ <https://mast.stsci.edu/tesscut>

Table 3. Candidate massive members of the Psc–Eri stream

#	<i>Gaia</i> DR2 ID	α (ICRS) [h:m:s]	δ (ICRS) [d:m:s]	$G_{\text{BP}} - G_{\text{RP}}$ [mag]	G [mag]	M_G [mag]	RV [km s ⁻¹]	Δv [km s ⁻¹]	$\Delta\mu$ [mas yr ⁻¹]	Δr [pc]	Name
1	3305012316783145728	04:00:40.81	+12:29:25.0	-0.008	3.387	-2.039	17.8	1.3	2.3	18.7	λ Tau ^a
2	2676509823708845056	22:03:18.87	-02:09:19.5	-0.083	4.622	-1.178	11.0	3.4	1.1	17.7	\circ Aqr ^b
3	5021010046848175616	02:04:29.45	-29:17:48.3	-0.193	4.638	-0.447	18.5	4.1	5.8	6.3	ν For ^c
4	2391220091406075648	23:44:12.11	-18:16:37.1	-0.080	5.185	-0.102	16.0	1.8	3.0	6.9	106 Aqr
5	2390144081839340288	23:51:21.37	-18:54:33.1	-0.153	5.125	0.096	12.7	2.9	0.3	0.9	108 Aqr ^d
6	2597327566122330880	22:47:42.80	-14:03:23.3	-0.037	5.666	0.481	15.0	3.9	1.19	11.4	τ^1 Aqr
7	2734781844037454592	22:24:00.51	+15:16:53.1	-0.085	6.764	0.503	5.0	2.8	0.9	14.6	HD 212442
8	2428341184508675456	00:14:54.54	-09:34:10.6	-0.103	5.747	0.531	19.9	3.9	0.7	11.8	HR 51
9	4878579825983429248	04:36:50.91	-30:43:00.3	-0.100	6.252	0.569	14.5	4.1	2.3	10.2	HR 1476
10	2746298781663140352	23:55:07.82	+07:04:15.2	-0.074	6.196	0.762	16.8	4.1	2.4	4.5	26 Psc
11	6549670305714644608	23:06:53.67	-38:53:32.2	0.054	5.631	0.921	11.9	3.1	2.0	17.5	ν Gru ^e
12	5045432364765457792	02:57:32.63	-38:11:27.2	-0.022	6.395	1.062	19.6	2.0	1.7	18.6	HR 893
13	2410222091875449216	23:09:49.58	-14:30:38.1	0.033	6.411	1.276	16.6	3.3	0.9	7.5	HR 8816
14	3252923090855768064	04:04:53.38	-02:25:37.8	-0.007	7.056	1.353	1.4	5.1	HD 25752
15	5175455696422545664	02:35:24.47	-09:21:02.8	0.016	7.097	1.445	19.1	1.6	3.4	8.8	HD 16152
16	3192744139408470272	04:21:35.19	-08:06:31.1	0.022	7.483	1.537	1.5	5.0	HD 27665
17	2982108287397220992	05:23:07.86	-17:13:26.1	0.064	8.250	1.567	0.7	6.2	HD 35308
18	2741090498161113344	00:15:57.32	+04:15:03.8	0.052	7.107	1.607	12.6	2.1	1.3	6.2	HD 1160 A ^f
19	2697317256631380736	21:58:36.60	+06:00:49.8	0.083	7.964	1.679	1.5	4.6	HD 208800
20	2721809496615333248	22:00:50.95	+07:51:08.5	0.070	7.989	1.713	1.2	3.8	HD 209105
21	2986248601510045184	05:00:01.23	-15:47:55.2	0.060	8.372	1.732	14.9	4.7	1.1	6.6	HD 32077
22	2542373597009506944	00:31:40.77	-01:47:37.4	0.094	7.041	1.776	1.0	5.2	HD 2830
23	2971453886581625600	05:36:04.99	-16:51:45.1	0.105	8.561	1.783	0.8	11.5	HD 37190
24	2391000395239148672	23:52:39.91	-18:33:42.8	0.122	6.804	1.806	13.0	2.9	0.9	0.1	HD 223785
25	5127759431765387392	02:45:18.39	-20:24:05.9	0.058	7.106	1.827	0.3	3.1	HD 17224
26	2982652206352410624	05:12:33.00	-17:27:16.5	0.117	8.514	1.899	1.8	6.2	HIP 2427
27	2982652275071888128	05:12:29.72	-17:27:08.9	0.119	8.564	1.961	0.7	6.7	HD 33857
28	3182650382147268992	05:07:44.10	-09:51:53.5	0.212	8.717	2.137	13.9	3.5	0.5	13.3	HD 33126 ^e
29	5145324782854148096	02:13:19.11	-14:54:27.3	0.495	7.556	2.226	19.0	3.1	9.3	8.1	HD 13722
30	3185719600136840064	04:35:06.82	-08:41:36.6	0.273	8.538	2.327	1.3	6.7	HD 29152
31	3300937801567693824	04:15:00.92	+10:44:53.1	0.283	7.652	2.385	16.0	2.1	3.1	18.6	HD 26843
32	2736194815262723712	22:34:06.27	+16:01:27.2	0.318	8.886	2.549	8.2	2.5	0.4	14.7	HD 213838
33	5155416822128110208	03:18:13.96	-13:49:45.4	0.303	8.226	2.625	1.7	2.0	HD 20573
34	3175513589608066048	04:19:34.07	-15:10:11.8	0.415	8.999	2.927	19.5	2.6	2.8	3.6	HD 27467 ^e

NOTE—Columns—# is the row number, sorted by M_G ; α (ICRS, epoch 2015.5), δ (ICRS, epoch 2015.5), $(G_{\text{BP}} - G_{\text{RP}})$, G , and $M_G = G - 5 \log_{10}(100/\varpi)$ from *Gaia* DR2; radial velocity obtained from SIMBAD; Δv is the absolute deviation of UVW velocities from the stream’s median value (km s⁻¹); $\Delta\mu$ is minimum difference in proper motion relative to the nearest neighbor in the Meingast et al. (2019) list (mas yr⁻¹); ΔXYZ : the physical distance (pc) to the nearest Meingast et al. (2019) member; common aliases. Notes on particular stars from SIMBAD are provided below.

^a Algol-type EB

^b Be star

^c α^2 CVn variable

^d Peculiar composition

^e Binary or multiple star

^f HD 1160 has two low-mass companions (Nielsen et al. 2012)—HD 1160 C is an M3.5 dwarf (*Gaia* DR2 2741090498159705216), and HD 1160 B is a brown dwarf candidate with an estimated mass of 39–166 M_{Jup} (Maire et al. 2016), 35–90 M_{Jup} , and 70–90 M_{Jup} (Garcia et al. 2017), depending on the age of the host star. Interpolating the 125 ± 15 Myr evolutionary models from Baraffe et al. (2015) at the Garcia et al. (2017) temperature ($T_{\text{eff}} = 3050 \pm 50$ K) and luminosity, corrected with the *Gaia* DR2 parallax ($\log L/L_{\odot} = -2.59 \pm 0.05$ dex, we infer a mass $M_B = 0.12 \pm 0.01 M_{\odot}$ ($\approx 123 M_{\text{Jup}}$). This is greater than the hydrogen-burning limit and indicates that HD 1160 B is probably a very-low-mass star and not a brown dwarf.

- Brasseur, C., Phillip, C., Fleming, S. W., Mullally, S., & White, R. L. 2019, *Astrocut: Tools for creating cutouts of TESS images*, , , ascl:1905.007
- Bressan, A., Marigo, P., Girardi, L., et al. 2012, *MNRAS*, 427, 127
- Brewer, J. M., Fischer, D. A., Valenti, J. A., & Piskunov, N. 2016, *ApJS*, 225, 32
- Cantat-Gaudin, T., Jordi, C., Vallenari, A., et al. 2018, *A&A*, 618, A93
- Clark, P. C., Bonnell, I. A., Zinnecker, H., & Bate, M. R. 2005, *MNRAS*, 359, 809
- Cranmer, S. R., & Saar, S. H. 2011, *ApJ*, 741, 54
- Cropper, M., Katz, D., Sartoretti, P., et al. 2018, arXiv e-prints, arXiv:1804.09369
- Cummings, J. D., Deliyannis, C. P., Maderak, R. M., & Steinhauer, A. 2017, *AJ*, 153, 128
- Cummings, J. D., & Kalirai, J. S. 2018, *AJ*, 156, 165
- Curtis, J. L. 2016, PhD thesis, Penn State University
- . 2017, *AJ*, 153, 275
- Curtis, J. L., Agüeros, M. A., Douglas, S. T., & Meibom, S. 2019, arXiv e-prints, arXiv:1905.06869
- Curtis, J. L., Wolfgang, A., Wright, J. T., Brewer, J. M., & Johnson, J. A. 2013, *AJ*, 145, 134
- Dahm, S. E. 2015, *ApJ*, 813, 108
- de Zeeuw, P. T., Hoogerwerf, R., de Bruijne, J. H. J., Brown, A. G. A., & Blaauw, A. 1999, *AJ*, 117, 354
- Dias, W. S., Alessi, B. S., Moitinho, A., & Lépine, J. R. D. 2002, *A&A*, 389, 871
- Douglas, S. T., Agüeros, M. A., Covey, K. R., & Kraus, A. 2017, *ApJ*, 842, 83
- Douglas, S. T., Curtis, J. L., Agüeros, M. A., et al. 2019, arXiv e-prints, arXiv:1905.06736
- Fingerhut, R. L., Lee, H., McCall, M. L., & Richer, M. G. 2007, *ApJ*, 655, 814
- Freeman, K., & Bland-Hawthorn, J. 2002, *ARA&A*, 40, 487
- Gaia Collaboration, Brown, A. G. A., Vallenari, A., et al. 2018a, *A&A*, 616, A1
- Gaia Collaboration, Babusiaux, C., van Leeuwen, F., et al. 2018b, *A&A*, 616, A10
- Gaidos, E., Mann, A. W., Rizzuto, A., et al. 2017, *MNRAS*, 464, 850
- Gallet, F., & Bouvier, J. 2015, *A&A*, 577, A98
- Garcia, E. V., Currie, T., Guyon, O., et al. 2017, *ApJ*, 834, 162
- Gossage, S., Conroy, C., Dotter, A., et al. 2018, ArXiv e-prints, arXiv:1804.06441
- Han, E., Curtis, J. L., & Wright, J. T. 2016, *AJ*, 152, 7
- Hodgkin, S. T., Pinfield, D. J., Jameson, R. F., et al. 1999, *MNRAS*, 310, 87
- Katz, D., Sartoretti, P., Cropper, M., et al. 2018, arXiv e-prints, arXiv:1804.09372
- Kharchenko, N. V., Piskunov, A. E., Röser, S., Schilbach, E., & Scholz, R. 2005, *A&A*, 438, 1163
- Kraus, A. L., Shkolnik, E. L., Allers, K. N., & Liu, M. C. 2014, *AJ*, 147, 146
- Landsman, W. B. 1993, in *Astronomical Society of the Pacific Conference Series*, Vol. 52, *Astronomical Data Analysis Software and Systems II*, ed. R. J. Hanisch, R. J. V. Brissenden, & J. Barnes, 246
- Lortet, M.-C., Borde, S., & Ochsenbein, F. 1994, *A&AS*, 107, 193
- Madsen, S., Dravins, D., & Lindegren, L. 2002, *A&A*, 381, 446
- Maire, A.-L., Bonnefoy, M., Ginski, C., et al. 2016, *A&A*, 587, A56
- Mamajek, E. E., & Hillenbrand, L. A. 2008, *ApJ*, 687, 1264
- Mann, A. W., Feiden, G. A., Gaidos, E., Boyajian, T., & von Braun, K. 2015, *ApJ*, 804, 64
- Matt, S. P., Brun, A. S., Baraffe, I., Bouvier, J., & Chabrier, G. 2015, *ApJL*, 799, L23
- Meibom, S., Mathieu, R. D., & Stassun, K. G. 2009, *ApJ*, 695, 679
- Meibom, S., Mathieu, R. D., Stassun, K. G., Liebesny, P., & Saar, S. H. 2011a, *ApJ*, 733, 115
- Meibom, S., Barnes, S. A., Latham, D. W., et al. 2011b, *ApJL*, 733, L9
- Meibom, S., Torres, G., Fressin, F., et al. 2013, *Nature*, 499, 55
- Meingast, S., & Alves, J. 2019, *A&A*, 621, L3
- Meingast, S., Alves, J., & Fürnkranz, V. 2019, *A&A*, 622, L13
- Michalik, D., Lindegren, L., & Hobbs, D. 2015, *A&A*, 574, A115
- Molenda-Żakowicz, J., Arentoft, T., Frandsen, S., & Grundahl, F. 2009, *AcA*, 59, 69
- Morris, B. M., Curtis, J. L., Douglas, S. T., et al. 2018, *AJ*, 156, 203
- Nielsen, E. L., Liu, M. C., Wahhaj, Z., et al. 2012, *ApJ*, 750, 53
- Oh, S., Price-Whelan, A. M., Hogg, D. W., Morton, T. D., & Spergel, D. N. 2017, *AJ*, 153, 257
- Önehag, A., Korn, A., Gustafsson, B., Stempels, E., & Vandenberg, D. A. 2011, *A&A*, 528, A85
- Pecaut, M. J., & Mamajek, E. E. 2016, *MNRAS*, 461, 794
- Preibisch, T., & Mamajek, E. 2008, *The Nearest OB Association: Scorpius-Centaurus (Sco OB2)*, ed. B. Reipurth, 235
- Press, W. H., & Rybicki, G. B. 1989, *ApJ*, 338, 277

- Rebull, L. M., Stauffer, J. R., Bouvier, J., et al. 2016a, *AJ*, 152, 113
- . 2016b, *AJ*, 152, 114
- Ricker, G. R., Winn, J. N., Vanderspek, R., et al. 2015, *Journal of Astronomical Telescopes, Instruments, and Systems*, 1, 014003
- Sandquist, E. L., Jessen-Hansen, J., Shetrone, M. D., et al. 2016, *ApJ*, 831, 11
- Sarro, L. M., Bouy, H., Berihuete, A., et al. 2014, *A&A*, 563, A45
- Scargle, J. D. 1982, *ApJ*, 263, 835
- Soderblom, D. R. 2010, *ARA&A*, 48, 581
- Soderblom, D. R., Laskar, T., Valenti, J. A., Stauffer, J. R., & Rebull, L. M. 2009, *AJ*, 138, 1292
- Soubiran, C., Jasniewicz, G., Chemin, L., et al. 2013, *A&A*, 552, A64
- Stauffer, J., Rebull, L., Bouvier, J., et al. 2016, *AJ*, 152, 115
- Stauffer, J. R., Schultz, G., & Kirkpatrick, J. D. 1998, *ApJL*, 499, L199
- Taylor, B. J. 2006, *AJ*, 132, 2453
- Torres, C. A. O., Quast, G. R., Melo, C. H. F., & Sterzik, M. F. 2008, *Young Nearby Loose Associations*, ed. B. Reipurth, 757
- Torres, G., Curtis, J. L., Vanderburg, A., Kraus, A. L., & Rizzuto, A. 2018, *ApJ*, 866, 67
- van Saders, J. L., & Pinsonneault, M. H. 2013, *ApJ*, 776, 67
- Wenger, M., Ochsenbein, F., Egret, D., et al. 2000, *A&AS*, 143, 9
- Wright, N. J., & Mamajek, E. E. 2018, *MNRAS*, 476, 381